$CO_2$ Inclusion in Crystals

# Carbon Dioxide Inclusion Phases of a Transformable 1D Coordination Polymer Host $[Rh_2(O_2CPh)_4(pyz)]_n$**

*Satoshi Takamizawa,* Ei-ichi Nakata, Haruhiko Yokoyama, Katsura Mochizuki, and Wasuke Mori*

Many inclusion compounds have been reported and the inclusion phenomenon has gained recognition in organic, inorganic, and physical chemistry, biology, and other branches of science.[1] The design and control of porous-network structures of extended inorganic frameworks has been extensively studied in recent years because of the ability to control their guest-adsorbing functionality.[2] The recent increase in the research of single-crystal host solids constructed by noncovalent intermolecular interactions is due to their specific properties such as guest exchange, gas storage, and transformation.[3] However, the mechanisms by which the guest invades the crystal host and by which the crystal transforms during the inclusion process are poorly understood.

An empty single-crystal host of rhodium(II) benzoate pyrazine, $[Rh^{II}_2(O_2CPh)_4(pyz)]_n$ (**1**), was prepared by a method reported elsewhere.[4] The component chains found in crystals of **1** adopt a perfectly linear geometry with the chain skeleton bridged by the pyrazine group in the axial direction of the well-known lanternlike core[5] of dinuclear rhodium benzoate (Figure 1). The polymeric chains are densely packed to form the crystal. The crystallographic data collected under different conditions are summarized in Table 1.

The crystal structure of **1** at 20 °C is shown in Figures 2 a, b, and c. The complex crystallizes in the monoclinic space group $C2/m$; there are no channel structures sufficient to hold guest molecules, but rather there are empty cages with dimensions of $9 \times 4 \times 3$ Å, with narrow gaps of approximately 1 Å found at

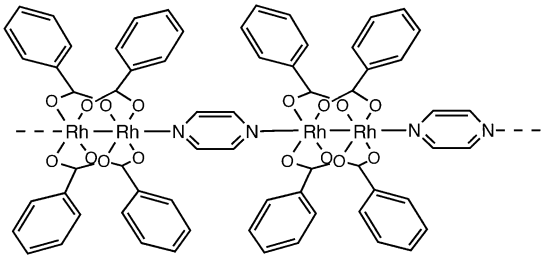


***Figure 1.*** Schematic drawing of the chain structure of compound **1**.

***Table 1:*** Crystallographic parameters of **1** under various conditions.

| | no $CO_2$ (Si oil) | no $CO_2$ (Si oil) | $CO_2$ | $CO_2$ | $CO_2$ |
|---|---|---|---|---|---|
| $CO_2$ molecules included | – | – | 0 | 0.733[a] | 3.0 |
| Phase | α | γ | α | β | β |
| $M$ | 770.36 | 770.36 | 770.36 | 802.62 | 902.39 |
| Crystal system | Monoclinic | Monoclinic | Monoclinic | Triclinic | Triclinic |
| Space group (number) | $C2/m$(no. 12) | $C2/c$(no. 15) | $C2/m$(no. 12) | $P\bar{1}$ (no. 2) | $P\bar{1}$ (no. 2) |
| $T$ [K] | 293.2 | 93.2 | 293.2 | 213.2 | 93.2 |
| $a$ [Å] | 17.821(9) | 17.42(3) | 17.85(1) | 9.577(3) | 9.556(3) |
| $b$ [Å] | 9.605(5) | 9.55(1) | 9.465(5) | 10.306(3) | 10.318(4) |
| $c$ [Å] | 12.362(8) | 19.70(4) | 14.113(9) | 10.850(4) | 11.079(5) |
| $\alpha$ [°] | 90 | 90 | 90 | 72.28(3) | 70.18(3) |
| $\beta$ [°] | 127.53(4) | 98.05(6) | 137.20(2) | 65.31(3) | 66.12(3) |
| $\gamma$ [°] | 90 | 90 | 90 | 63.25(2) | 63.02(3) |
| $V$ [Å] | 1678(1) | 3244(9) | 1620(1) | 859.9(5) | 873.7(6) |
| $Z$ | 2 | 4 | 2 | 1 | 1 |
| $D_{calcd}$ [g cm$^{-3}$] | 1.524 | 1.577 | 1.579 | 1.550 | 1.715 |
| μ [cm$^{-1}$] | 10.30 | 10.66 | 10.67 | 10.12 | 10.15 |
| Final $R_1$ ($I > 2\sigma(I)$) | 0.0359 | 0.0613 | 0.0869 | 0.0896 | 0.1031 |
| $WR_2$ (all data) | 0.0746 | 0.1183 | 0.2481 | 0.2350 | 0.2504 |
| GOF on $F^2$ | 1.044 | 1.048 | 1.165 | 1.131 | 1.367 |

[a] The incorporated $CO_2$ molecules were detected only on the crystallographic A site with an occupation probability of 73.3 % (See Figure 3).

[*] Dr. S. Takamizawa, E.-i. Nakata, Prof. Dr. H. Yokoyama, Prof. Dr. K. Mochizuki
Graduate School of Integrated Science
Yokohama City University
Kanazawa-ku, Yokohama, Kanagawa 236-0027 (Japan)
Fax: (+81) 45-787-2187
E-mail: staka@yokohama-cu.ac.jp
Prof. Dr. W. Mori
Department of Chemistry
Faculty of Science, Kanagawa University
Tsuchiya, Hiratsuka
Kanagawa 259–1293 (Japan)

[**] We thank Dr. M. Shiro and Dr. A. Kishi (Rigaku Corp.) for their technical assistance with the X-ray measurements; pyz = pyrazine.

Supporting information for this article is available on the WWW under http://www.angewandte.org or from the author.

 DOI: 10.1002/ange.200351368  

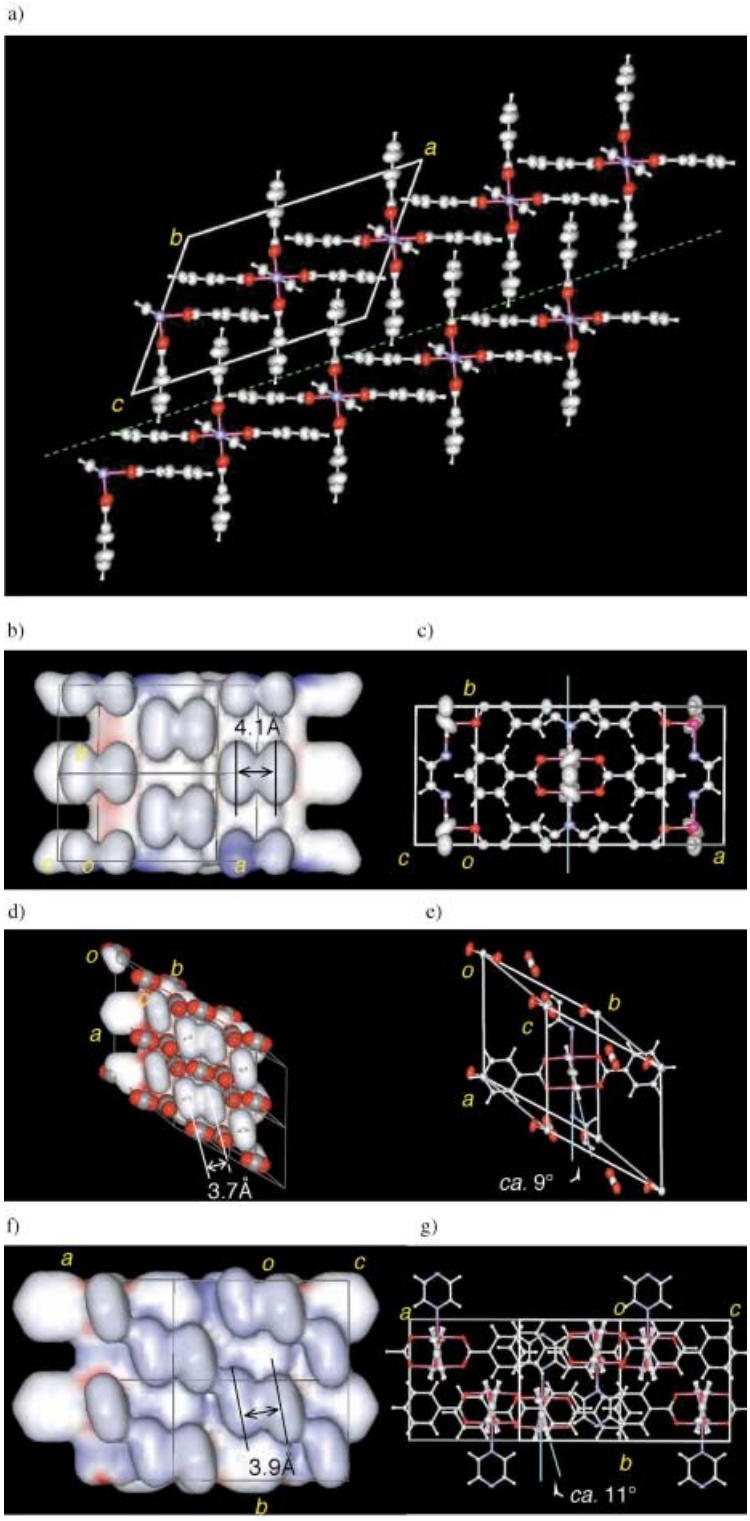


***Figure 2.*** Views of crystal **1**: a) view along the chain vector showing thermal ellipsoids for the crystal structure in $CO_2$ atmosphere at 20 °C; b) surface view along the dashed-green cross section of a); c) the corresponding ellipsoidal view; d) surface view of the $CO_2$-inclusion state at −180 °C; e) the corresponding ellipsoidal view; f) surface view of the crystal under conditions where $CO_2$ was absent at −180 °C ; g) the corresponding ellipsoidal view. Atoms: Rh (magenta), C (grey), H (white), N (blue), O (red). All ellipsoidal views are shown at 50% probability.

their four corners,[6] which are formed by the benzene rings of benzoate moieties arranged parallel to the chain vector. On cooling samples in a $CO_2$ atmosphere, the crystal underwent a phase transition to a new structure adopting the triclinic space group $P\bar{1}$, and generating one-dimensional (1D) channels (Figure 2d). The cages are transformed into channels by a slippage of the chain skeletons along the chain vector; the benzene ring tilts 9° away from the chain vector (Figure 2e). External $CO_2$ is incorporated into the channels in the form of molecular wires, in which the molecular axes of the $CO_2$ molecules are almost parallel and perpendicular to the channel direction at sites A and B, respectively (Figure 3).

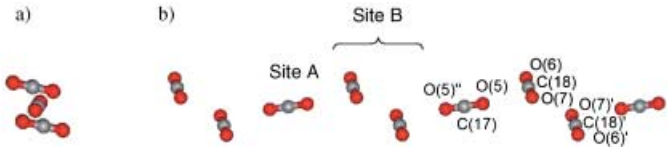


***Figure 3.*** Ball-and-stick representation of the column of $CO_2$ molecules in the channels of crystal **1** in the inclusion state: a) top view and b) side view. Pertinent atomic separations [Å] and angles [°]: O(5)-C(18) 2.85, C(18)-C(18)′ 3.53, C(18)-O(6)′ 4.13, C(18)-O(7)′ 3.17; C(17)-C(18)-C(18)′ 124.6, C(17)-O(5)-C(18) 162.3, O(5)-C(18)-O(6) 90.4, O(5)-C(18)-O(7) 92.3.

Evidence for the diffusion of gas into the crystal through the narrow gaps at the corners of the cages was obtained from sorption measurements. The $CO_2$ adsorption isotherm at 0 °C demonstrated that gas was smoothly incorporated into the crystal with a Langmuir-type curve due to monolayer adsorption (see Supporting Information). The estimated Brunauer–Emmett–Teller (BET) surface area is extremely large at 274.1 $m^2 g^{-1}$,[7] which indicates that the $CO_2$ gas is adsorbed not on the crystal surface but also inside the crystal. The accumulated quantity of $CO_2$ gas at ambient pressure is 23.7 $cm^3(STP)\,g^{-1}$ or 37.4 $cm^3(STP)\,cm^{-3}$ (where $cm^3(STP)$ represents the volume of gas accumulated under standard conditions). This corresponds to an average of 0.81 $CO_2$ molecules per $Rh_2$ unit or per cage. The $CO_2$ sorption isobar measurement at ambient pressure yielded a monotonous desorption curve with a saturation point at approximately −80 °C (Figure 4). The saturated quantity of 3.0 molecules per $Rh_2$ unit at −80 °C agrees well with the composition determined from the single crystal X-ray diffraction data at −180 °C. The crystal structures at 20 °C and −60 °C should also contain the observed amount of ≈0.5 and 2.9 $CO_2$ molecules per $Rh_2$ unit, respectively, but the molecules could not be located by X-ray crystallography, probably due to their thermal motion. The unit-cell volume in a $CO_2$ atmosphere at 20 °C decreased by 3% in comparison with that measured under conditions where $CO_2$ is absent, which implies that stressed $CO_2$ inside the lattice attempts to deform the cages (Table 1).

Simultaneous powder X-ray diffraction (XRD) and differential scanning calorimetry (DSC) measurements were conducted. On cooling, changes were observed in

  

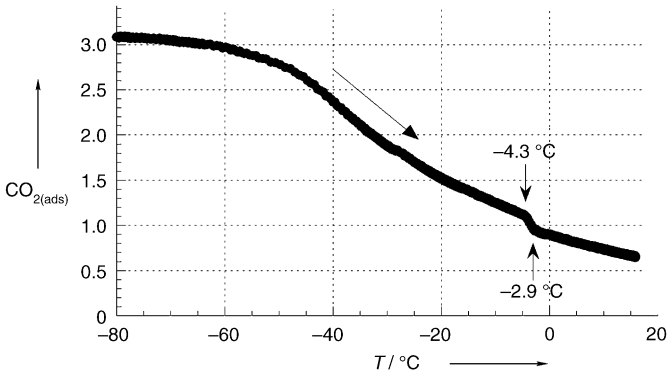


***Figure 4.*** Isobar curve at ambient $CO_2$ pressure (gravimetric method) using a Cahn 2000 electronic balance ($CO_{2(ads)}$ = moles of $CO_2$ adsorbed per $Rh_2$ unit).

the diffraction pattern of **1** and the peaks in the XRD patterns decreased in intensity and sharpness near −10 °C, with a corresponding exothermic peak in the DSC trace (Figure 5a), which clearly shows that a structural rearrangement takes place in the region of the phase transition. At lower temperatures, the peaks in the new diffraction patterns became sharper and increased in intensity. This property indicates that the bulk-phase transition occurs at this temperature; no significant changes took place under a nitrogen atmosphere (see Supporting Information). The patterns at 20 °C and −70 °C are in good agreement with those simulated using the crystal structures under $CO_2$ atmosphere with space groups $C2/m$ (at 20 °C) and $P\bar{1}$ (at −180 °C), respectively (see Supporting Information). In the scanning temperature range of 50 to −40 °C, the DSC measurements repeatedly revealed exo- and endothermic phase transitions at −9.9 °C (cooling) and −4.6 °C (heating) in a $CO_2$ atmosphere at ambient pressure (Figure 5b), while no peaks were observed when a purely nitrogen atmosphere was used. The transition enthalpy ($\Delta H$) of crystal **1** in a $CO_2$ atmosphere, calculated from the areas of the DSC peaks, is −5.8 (cooling) and 5.4 (heating) kJ mol$^{-1}$ with respect to the $Rh_2$ units. The temperatures where the sets of cyclic DSC peaks occur shift to lower values as the concentration of $CO_2$ decreases. The natural logarithm of the partial pressure ($\ln P_{CO2}$) and the reciprocal transition temperature ($T^{-1}$) show a good linear correlation (Figure 5c). This correlation coincides with the Clausius–Clapeyron equation, which is commonly used for estimating differentials in the isosteric heat of adsorption from pressure and temperature data measured at the same adsorption levels:

$$\text{gas} + \text{adsorbent} \rightarrow \text{gas on adsorbent} \quad (1)$$

$$\mathrm{d}(\ln P)/\mathrm{d}(T^{-1}) = \Delta H/\mathrm{R} \quad (2)$$

where R and $\Delta H$ denote the gas constant and the adsorption enthalpy of gas, respectively. This relationship indicates that the amounts of $CO_2$ adsorbed by **1** are the same at the phase transition points, and $-\Delta H$ is the isosteric heat of adsorption ($-\Delta H_{iso}$). The estimated value of $\Delta H_{iso}$ for $CO_2$ is determined from the gradient to be −34.5 kJ mol$^{-1}$ (cooling or adsorption) and 39.6 kJ mol$^{-1}$ (heating or desorption). Similar

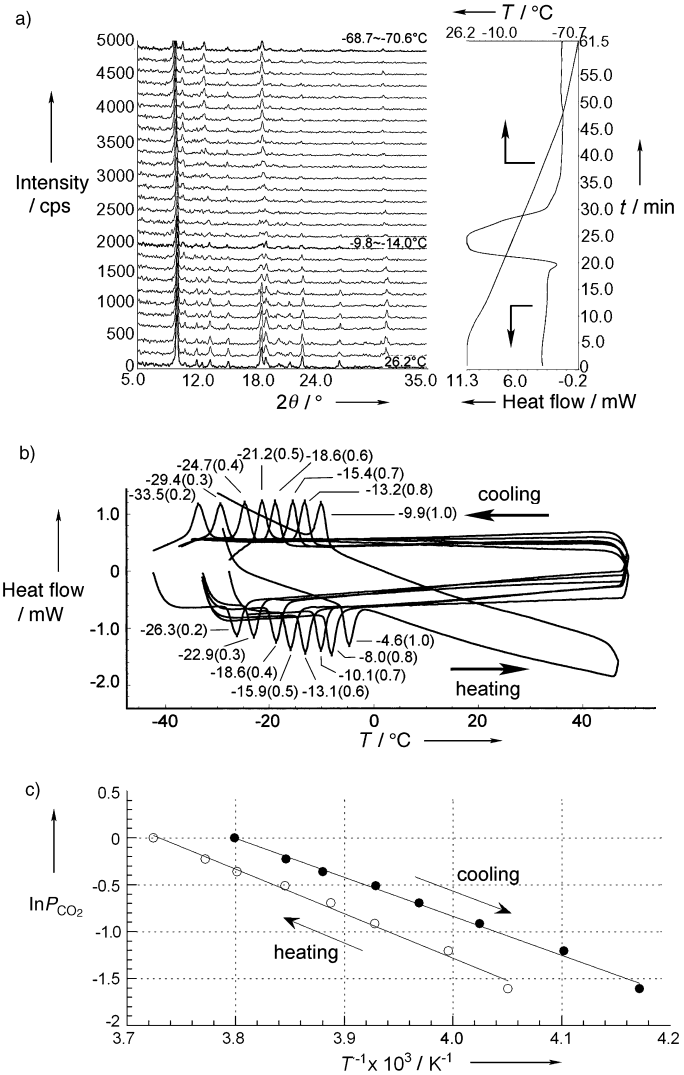


***Figure 5.*** a) X-ray diffraction patterns of crystal **1** in a $CO_2$ atmosphere as a function of temperature, with a simultaneous DSC measurement; b) independent DSC cyclic patterns of crystal **1** under ambient pressure with different $CO_2/N_2$ mixtures (values on the curves denote temperatures at the peak maxima with the $CO_2$ contents shown in parentheses); c) correlation between the partial pressure of $CO_2$ and the transition temperature. Simultaneous XRD/DSC measurements were recorded on a Rigaku XRD-DSC II diffractometer with a temperature scan rate of 3 °C min$^{-1}$ and a 2-$\theta$ scan rate of 15 ° min$^{-1}$ over the range 5 to 35° with $Cu_{K\alpha}$ radiation ($\lambda$ = 1.54184 Å). Independent DSC measurements at a scanning rate of 5 °C min$^{-1}$ were recorded on a Shimadzu DSC-60 calorimeter.

behavior has been observed for a copper derivative of compound **1**.[8] The critical quantity of adsorbed $CO_2$ is estimated to be one $CO_2$ molecule per $Rh_2$ unit at a significant transition point close to −5 °C from the isobar (Figure 4b). The estimated value indicates that the $C2/m$ crystal can include no more than one $CO_2$ molecule under the current "α saturation" condition and subsequently transforms to the inclusion crystal, which enables up to three $CO_2$ molecules per $Rh_2$ unit, contained within the channels.

Under conditions in which $CO_2$ is absent, the space-group symmetry changes from $C2/m$ to $C2/c$ on cooling to −180 °C,

  

and the crystal exhibits a channel structure with a narrow neck of ≈2 Å diameter, which is too narrow for atmospheric gas to be adsorbed (Figure 2 f and g). However, the *C2/c* crystal can smoothly adsorb $N_2$ gas in the microporous region at 77 K with a large BET surface area of 352.5 $m^2 g^{-1}$,[4] where it is likely that the gas sorption process involves a crystal transformation, at least on a local scale.

The cage α phase (*C*2/*m*) is replaced by the inclusion β phase below the transition point in the presence of $CO_2$ gas. It is known that an offset stacking configuration is energetically more stable than that of a perfect overlap.[9] From the perspective of crystal energy, therefore, on depressing thermal vibration as the temperature decreases, a perfect face-to-face overlap of the benzene planes in the α phase changes to an offset configuration with tilting of the rings in phases β ($P\bar{1}$) and γ (*C*2/*c*) favored, where the separation distances of the planes are approximately 4.1, 3.7, and 3.9 Å in the α, β, and γ phases, respectively. It is noted that the two modes of chain slippage and offset stacking clearly occur simultaneously in the inclusion β phase. They regulate the formation of the inclusion crystal and shorten the interplanar distances, which may allow the volume of space in the channels to be maximized and the crystal to be stabilized. In fact, temperature and pressure are critical to the understanding of the entire transition process.

This inclusion process results in a smooth and reversible transformation from an "empty single crystal" to an "inclusion single crystal" without the exchange of guests. This reversible control of the inclusion process with the remarkable ability to coherently crystallize light guest species from a gaseous environment will open the door to many new techniques.

## Experimental Section

Single-crystal X-ray diffraction data was collected alternatively in a $CO_2$ atmosphere and in the absence of $CO_2$ by sealing a glass capillary containing the sample and $CO_2$ gas at ambient pressure and by scooping on a cryoloop through silicone oil, respectively. All experiments were performed on a Rigaku RAXIS RAPID imaging plate diffractometer with a nitrogen-flow temperature controller and $Mo_{K\alpha}$ radiation ($\lambda = 0.71073$ Å) over a temperature range of 20 to −180 °C. Empirical absorption corrections were applied using the ABSCOR program. The structures were solved by the Patterson method (DIRDIF94 PATTY) and refined by full-matrix least-squares on $F^2$ (SHELXL97). Non-hydrogen atoms were refined anisotropically, while hydrogen atoms were fixed at calculated positions and refined using a riding model. CCDC-19524, 19525, 194691, 194692, and 194693 contain the supplementary crystallographic data for this paper. These data can be obtained free of charge via www.ccdc.cam.ac.uk/conts/retrieving.html (or from the Cambridge Crystallographic Data Centre, 12, Union Road, Cambridge CB2 1EZ, UK; fax: (+44) 1223-336-033; or deposit@ccdc.cam.ac.uk).

Received: March 11, 2003
Revised: July 14, 2003 [Z51368]

**Keywords:** adsorption · host–guest systems · inclusion compounds · phase transitions · X-ray diffraction

[1] a) *Inclusion Compounds, Vol. 4* (Eds.: J. L. Atwood, J. E. D. Davies, D. D. MacNicol), Oxford University Press, Oxford, **1991**; b) *Topics in Inclusion Science, Vol. 2* (Eds.: T. Osawa, J. L. Atwood), Kluwer, Dordrecht, **1991**; c) *Host–Guest Complex Chemistry: Synthesis, Structures, Applications* (Eds.: F. Vögtle, E. Weber), Springer, Berlin, **1985**; d) *Comprehensive Supramolecular Chemistry, Vols. 1–11* (Eds.: J. L. Atwood, J. E. D. Davies, D. D. MacNicol, F. Vögtle), Elsevier Science, Oxford, **1996**; e) J. M. Lehn, *Supramolecular Chemistry: Concepts and Perspectives*, VCH, Weinheim, **1995**; f) L. R. Nassimbeni, *Acc. Chem. Res.*, in press.

[2] a) O. M. Yaghi, M. O'Keeffe, M. W. Ockwing, H. K. Chae, M. Eddaoudi, J. Kim, *Nature* **2003**, *423*, 705; b) E. J. Cussen, J. B. Claridge, M. J. Rosseinsky, C. J. Kepert, *J. Am. Chem. Soc.* **2002**, *124*, 9574; c) R. Kitaura, K. Seki, G. Akiyama, S. Kitagawa, *Angew. Chem.* **2003**, *115*, 444; *Angew. Chem. Int. Ed.* **2003**, *42*, 428; d) S. S.-Y. Chui, S. M.-F. Lo, J. P. H. Charmant, A. G. Orpen, I. D. Williams, *Science* **1999**, *283*, 1148; e) S. Takamizawa, M. Furihata, S. Takeda, K. Yamaguchi, W. Mori, *Macromolecules* **2000**, *33*, 6222.

[3] a) J. L. Atwood, L. J. Barbour, A. Jerga, *Science* **2002**, *296*, 2367; b) K. Biradha, Y. Hongo, M. Fujita, *Angew. Chem.* **2002**, *114*, 3545; *Angew. Chem. Int. Ed.* **2002**, *41*, 3395; c) J. L. Atwood, L. J. Barbour, A. Jerga, B. L. Schottel, *Science* **2002**, *298*, 1000.

[4] S. Takamizawa, T. Hiroki, E. Nakata, K. Mochizuki, W. Mori, *Chem. Lett.* **2002**, 1208.

[5] F. A. Cotton, R. A. Walton, *Multiple Bonds between Metal Atoms*, 2nd ed., Oxford University Press, New York, **1993**.

[6] The atomic void sizes were determined by subtracting van der-Waals radii of 3.0 Å from various distances between the non-hydrogen atoms of the aromatic rings.

[7] The $CO_2$ adsorption isotherm was measured on a Quantachrome AUTOSORB-1 at 0 °C with pressures ranging from $3 \times 10^{-3}$ to 1 atm (relative pressure = *P*(pressure)/$P_0$(saturated pressure), which ranged from $1 \times 10^{-4}$ to $3 \times 10^{-2}$). The BET surface area in a relative pressure range from 0.01 to 0.03 was estimated using the ASWin program package.

[8] S. Takamizawa, E. Nakata, H. Yokoyama, *Inorg. Chem. Commun.* **2003**, *6*, 763.

[9] C. A. Hunter, J. K. M. Sanders, *J. Am. Chem. Soc.* **1990**, *112*, 5525.

  